The Determination and Use of Orthometric Heights Derived from the Seasat Radar Altimeter over Land

*Chua P. K.**, *A. H. W. Kearsley*†, *J. K. Ridley*, *W. Cudlip*, and *C. G. Rapley*
Mullard Space Science Laboratory, University College London, Holmbury St. Mary, Dorking, Surrey RH5 6NT, United Kingdom

ABSTRACT: Orthometric height data derived from the Seasat radar altimeter are compared with ground control data based on terrestrial survey measurements in the Simpson Desert, Australia. A bicubic spline surface is used to model the ground control heights, and the RMS of the differences between the model surface and the raw measurements in an area containing the most trustworthy height control data is found to be about ± 0.4 m. We show that the altimetry recovers the mean terrain height with an accuracy slightly better than 1 m, and with a precision of ± 0.4 to ± 0.7 m per radar pulse. This implies a precision of about ± 0.05 to ± 0.08 m for the mean of an ~50 km profile. Given this capability, we suggest various applications of satellite radar altimetry over land, including the use of height data to validate and/or extend digital elevation models, to improve local geoid models, and to improve the satellite orbit ephemeris.

INTRODUCTION

RADAR ALTIMETRY FROM SATELLITES has been used extensively in geodetic and oceanographic studies. Because the instruments were designed specifically for operation over the open ocean, applications over land have been largely ignored. Nevertheless, of the three earth-orbiting radar altimetry missions flown to date—GEOS 3 (1975 to 1978), Seasat (1987), and Geosat (launched in 1985)—the Seasat altimeter alone produced some 10^7 echo waveforms from inland water and land during its three months of operation. Echoes were obtained from approximately 35 percent of Earth's inland water and land surfaces, and of these, 35 percent are easily interpretable in terms of surface height, roughness, and radar backscatter characteristics (Rapley *et al.*, 1987).

Research into the measurements obtained by the Seasat altimeter over flat terrain areas has illustrated applications over a wide variety of scientific areas, ranging from geology to climate research (Rapley *et al.*, 1987). Where free-standing water exists, this tends to dominate the surface backscatter, making hydrological measurements possible. Elsewhere, particularly over unvegetated or lightly vegetated arid lands, the measurements relate to the solid surface.

Given the large quantity of data available from the current Geosat altimeter mission, and the data anticipated from both the ERS-1 altimeter mission to be launched in 1991 and the Advanced Terrain Tracking Altimeter (RA-2) planned for the European Space Agency's (ESA) Polar Orbiting Platform (Andrewartha *et al.*, 1988), the accuracy, precision, and new applications of altimeter range measurements over land warrant special attention.

This paper describes research recently carried out at Mullard Space Science Laboratory (MSSL), University College London, to evaluate the precision and accuracy with which land surface heights can be recovered from the Seasat altimeter data. We compare altimeter-derived heights with ground surveyed height data and suggest factors which contribute to the observed differences. We also discuss applications of the data, including

- Validation and extension of Digital Terrain Models,
- Evaluation of high-order geoid models, and
- Evaluation and improvement of satellite radial orbit models.

In the following sections we review the basic principles of satellite altimetry, outline the study we carried out to test the capacity of the Seasat altimeter to recover heights of the terrain, describe and analyze the results, and provide a discussion of the possible applications of the technique.

FUNDAMENTALS AND BACKGROUND

MEASURING PRINCIPLES OF SATELLITE ALTIMETRY

A radar altimeter operates by measuring the time delay between the transmission of a brief pulse of radio waves and the receipt of its echo. The range value (R_m), corresponding to the time delay t_m, is given by

$$R_m = (c\ t_m)/2 \qquad (1)$$

where c is the propagation speed.

All altimeters to date have operated in the pulse-limited mode, in which the footprint size over a flat surface is determined by the transmitted pulse duration and not by the antenna beamwidth (Rapley *et al.*, 1987). The intercept of the one-way 3-dB response of the antenna with the ground defines the beam limited footprint (BLF), which in the case of Seasat was ~20km in diameter. The transmitted pulse propagates towards the ground as part of an expanding spherical shell. For a pulse-limited instrument, given a flat ground surface, a linearly growing disk-shaped surface patch is illuminated by the radio pulse when the shell intercepts the plane of the ground. This continues until the rear of the shell intercepts the plane of the ground, after which the illuminated patch grows as a constant-area annulus. The area illuminated by this expanding shell just prior to it changing to a constant area annulus defines the pulse limited footprint (PLF) to which the range measurement corresponds. The diameter of the (PLF) increases with increasing surface roughness, varying from ~2 to 9km for Seasat. Figure 1 shows the relationship between PLF and BLF over flat terrain.

* On leave from Laboratory for Image and Signal Processing, National University of Singapore, Lower Kent Ridge Road, Singapore 0511, Republic of Singapore.

† On leave from School of Surveying, University of New South Wales, P.O. Box 1, Kensington, NSW 2033, Australia.

PHOTOGRAMMETRIC ENGINEERING & REMOTE SENSING,
Vol. 57, No. 4, April 1991, pp. 437–445.

0099-1112/91/5704–437$03.00/0

Over a flat but tilted surface, the position of the PLF within the BLF depends on the regional slope, being centered at the nearest point to the altimeter (Figure 2). This introduces an error in the nadir height estimate known as slope-induced error, which can be corrected for, provided the regional slope is known.

At the altimeter, the echo is sampled at discrete intervals of delay time (range bins) over a finite delay period. This period corresponds to a range interval referred to as the range window. The Seasat altimeter had a range window with a range coverage of about 28 m. To synchronize the range window over the different returned echo delays due to varying range as the satellite progresses around its orbit, an on-board range tracker system is employed.

The Seasat tracker was designed to maintain the center of the range window, or the tracking point, over the 50 percent power point of the echo leading edge, corresponding to the mean surface elevation for ocean returns. The time corresponding to the position of the tracking point is used to define t_m.

Over land, where the range from the altimeter to the surface can change rapidly, the track point was often displaced from the 50 percent power point of the waveform leading edge, necessitating a correction known as retracking. Where the range tracker cannot maintain the returned echo within the range window (loss of lock), an acquisition sequence was activated to recapture the surface echoes and allow continuous tracking to resume.

Over topographic terrain (i.e., terrain with systematic, non-statistical height variations), pulse-limited altimetry breaks down, since it is not possible to relate an identifiable point on the return echo with the mean height at nadir. The limits on the characteristics of surface topography amenable for Pulse-limited observations are hard to define. However, the observation of sequences of "simple" echoes implies that the surface is flat and that useful information can be extracted.

Rapley *et al.* (1987) have shown that long sequences of "simple," ocean-like echoes are observed over many of the world's arid zones. They note a correlation between such areas and zones where the topographic variability is low. One such area lies within the Simpson Desert, Australia, bounded by $-24.5° \leq \varphi \leq -29.5°$ and $134.5° \leq \lambda \leq 139.5°$. This area is of particular interest, because it possesses a good coverage of ground survey data which can be used as control for the tests. It is also relatively flat. Figure 3 shows a map of topographic variability over the area used in this study. From the map, we expect that most of the heights in a 1° by 1° block in this region will vary by less than 200m and, along the ground track of LR81 (see Section 3.4), less than 100m. The area is a vast sandridge desert, characterized by long parallel lines of dunes, ranging from 15m in height to the west to 38m in the east and running for up to 200km in a SSE to NNW direction. The crests are regularly spaced in any one area, but swales range from 200m on the W edge of the desert to 2km in the E. The swales in the area of this study were 400 to 500m wide.

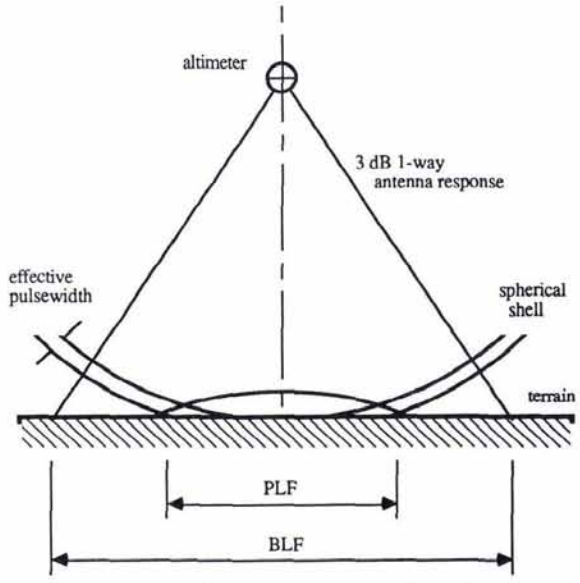

FIG. 1. Pulse limited footprint (PLF) versus band limited footprint (BLF).

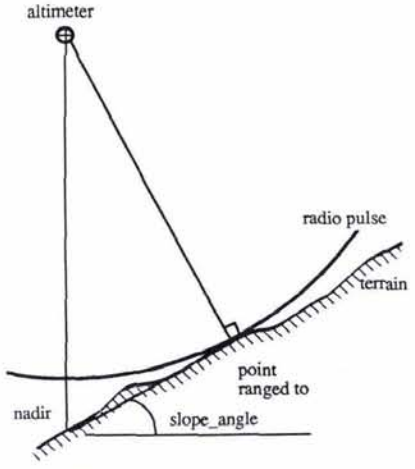

FIG. 2. Displacement of altimeter ranging point by sloping terrain.

HEIGHT REFERENCE SURFACES

The two surfaces commonly used for height reference are the ellipsoid and geoid. The geoid is the equipotential surface at

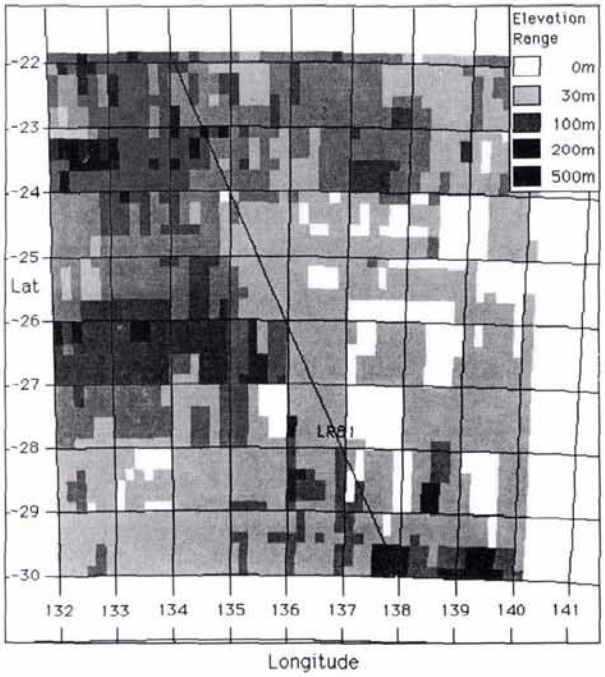

FIG. 3. Elevation Range Index Map for the Simpson Desert.

the mean sea level and is approximated by the mean sea surface level, as determined by tide gauges. Heights obtained from ground surveys are referenced to the geoid, because the local horizon used in the surveys is defined physically by a spirit bubble or a gravity-directed compensator. Such heights are called orthometric heights (H), and are the most useful in practice because they give the direction of the flow of water.

The simplest mathematical figure which describes the geoid is the ellipsoid, defined by its semi-major axis (a) and flattening (f) values. A height measured with respect to an ellipsoid is known as an ellipsoidal height, and is the parameter derived from satellite positioning (e.g., GPS) or altimetry. It is therefore necessary to transform a satellite-derived ellipoidal height to an orthometric height before any proper comparison can be made. The maximum departure of the geoid from the ellipsoid globally is about 100m.

Figure 4 shows the relationship between the two height systems. In this figure, the distance H corresponds to the orthometric height of the point P,N defines the geoidal undulation or geoid height, and is the distance between the geoid and the ellipsoid, and the ellipsoidal height of P is given by the quantity h (Heiskanen and Moritz, 1967, p. 83). The values of H,N and h are, for small deflections of the vertical (<20″), effectively measured along the ellipsoidal normal. The relationship between the three quantities is, therefore,

$$h = N + H \tag{2}$$

N is best determined by gravimetric means, e.g., by Stokes' integral or, to a fair approximation from geopotential models, expressed in terms of a spherical harmonic series. The integrity of the model in any area depends upon the quality of the geoid-related data in that area used in the evaluation of the potential coefficients, and the number of terms included in the series.

In this study, the geoid undulations were computed from the OSU86E geopotential mode, which is defined up to degree and order 360, i.e., its shortest half wavelength is about 55 km. It was based upon the GEM-L2 geopotential model, a satellite-only geopotential model defined to degree and order 20. Higher order terms were based upon 30 by 30′ mean gravity anomalies derived from land measurements in a some areas, including Australia, and from satellite altimetry over the oceans. Where no 30′ data existed, estimates of 1° by 1° mean gravity anomalies were used when available (Rapp and Cruz, 1986).

OSU86E has been shown to model the geoid in the area of interest with a relative error or better than 5 ppm (Kearsley and Holloway, 1988; 1989). In fact, detailed geoid studies using available gravity data show that it models the geoid surface to better than 2 ppm along the profiles in the tests. The geoid in this test area is quite featureless and slopes very evenly, dropping from 14.30m to 14.86m along the 50km of the LR81 profile, and from 15.21 to 14.56m along the 50km of R757. The contour of the geoid crosses the ground track fairly acutely (≈20°), which helps to explain why the geoid profile along the ground track is quite flat.

The reference ellipsoid used for both OSU86E and the orbit model (see next section) is defined by the Geodetic Reference System 1980 (GRS80), where a = 6,378,137 m and f = 1/298.257 223 563 (Moritz, 1980).

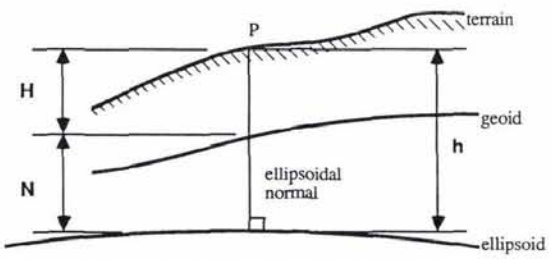

FIG. 4. Orthometric height (H), ellipsoidal height (h), and geoidal undulation (N).

DATA SETS AND METHODOLOGY

ESTIMATION OF ALTIMETER HEIGHTS FROM RANGES

The primary source of Seasat altimeter data used here was the Sensor Data Records (SDRs) provided by JPL. In order to derive meaningful surface height estimates from these, corrections have to be applied and additional information supplied. Thus, the generation of height profiles over the test area was carried out as follows:

(i) Orbit Ephemeris. A GEM-T1 orbit ephemeris was kindly provided by J. Marsh of the NASA Goddard Space Flight Center. This was derived using the Goddard Earth Model T1 (GEM-T1) gravity model, which is resolved to degree and order 36, and is based solely on ground tracking data of artificial satellites. Its solution used new and more precise laser data than earlier models and introduced consistent models for Earth and ocean tides, tidal deformations, etc., in a simultaneous solution. Marsh *et al* (1988) have shown that the consistency of altimeter heights at ocean crossover points is 50cm RMS. However, the absolute geocentric accuracy may be worse than this due to the presence of correlated errors in the ascending and descending track data at specific geographic locations. Also, analyses of crossover data over Africa, South America, Australia, and the Caspian Sea indicate that the performance over non-ocean areas is rather worse (~1m RMS. Guzkowska *et al.*, 1990).

(ii) Instrument Corrections. The instrument corrections (clock bias, internal delays, antenna phase center offset from the spacecraft centre of mass) were taken from the values provided by JPL in the GDR data tapes (Jet Propulsion Lab, 1980b). A datation bias correction associated with the SDR echo data was applied when deriving the nadir coordinates from the orbit ephemeris.

(iii) Refraction Corrections. Corrections for ionospheric and atmospheric refraction effects were also derived from the JPL GDR data tapes. No interpolation was carried out because the values change slowly. No correction was applied for liquid water in the troposphere because the presence of liquid water over the Simpson Desert is unlikely.

(iv) Echo Retracking. The Seasat altimeter tried to maintain the leading edge of the return echoes at the center of its range window (the tracking point). Each echo was digitized using 60 bins, each with an effective range of 0.47m. Over non-ocean surfaces the tracker was often unable to maintain the leading edge of the return at the tracking point; in order to estimate the true range to the surface, the offset of the leading edge from the middle of the range window has to be measured during a process called retracking.

Ideally, retracking would determine the offset between the tracking point and the position on the leading-edge of the waveform corresponding to the mean surface height. After some testing of techniques, we chose to retrack using a threshold retracking technique which determines the first location on the leading edge of the 50 percent power point. We take the power to be represented by the "amplitude" of the waveform, as described below. This has the advantage that it makes no *a priori* assumptions about the nature of the observed surface, and gives consistent results for noisy non-ocean-like waveforms. The disadvantage is that it can introduce bias into the surface height although, for waveforms with simple shapes, estimates of the bias can be made and, for complex waveforms, the effect of the

bias is negligible in light of the additional uncertainties in interpreting the measurements (Ridley, 1989).

Before retracking we characterize the shape of the waveform using two parameters, amplitude and width, in the manner described by Wingham *et al.* (1986). The amplitude is defined as twice the height of the vertical center of gravity of the waveform. The "width" is the width of a box whose height equals the waveform amplitude and whose area equals the area of the waveform.

(v) Surface Bias Corrections. Field data of the Simpson test sites (Guzkowska *et al*, 1989) provided the basis for a statistical model of the distribution of heights, slopes, and variation of slope with height corresponding to the ocean-like echoes observed over the areas of parallel longitudinal dunes. Waveforms generated from these model surfaces provided an excellent fit to the observed waveforms. Using these idealized waveforms, the difference between the elevation measured at the retrack point on the waveform leading edge and the true mean surface was estimated to be 52 ± 10cm. In addition, information on the distribution of surface slopes with height was used to determine the electromagnetic bias which arises from the fact that the surface slopes are not independent of height. The slopes are greater the greater the elevation. Thus, the small scale roughness defines the polar response of the surface and the slopes define the power that is returned from the various heights. The half-power point on the leading edge is no longer the mean surface and the bias introduced is evaluated at 0.24m.

From the above a corrected range value, R_c, was derived from the measured range value R_m recorded on the SDR tape using the sum of the above range corrections δR: i.e.,

$$R_c = R_m + \delta R \tag{3}$$

An estimate of the surface orthometric height (H_{alt}) was then made from R_c using the knowledge of the satellite height above the reference ellipsoid (h_{sat}), the correction for Earth tides (Δh_{Etide}) taken from the GDRs, and the geoidal undulation at the nadir point derived from the geopotential model (N_{model}): i.e.,

$$\begin{aligned} H_{alt} &= h_{sat} - [(R_c S) + \Delta h_{Etide} + N_{model}] \\ &= h_{sat} - [(R_m + \delta R)S + \Delta h_{Etide} + N_{model}] \end{aligned} \tag{4}$$

where S is the slope correction factor, defined here to first order as

$$S = 1/\cos(\text{slope angle}). \tag{5}$$

For the Seasat altimeter, the slope-induced height error is 1.2m for a 0.1 degree slope (gradient 1.8×10^{-3}). The correction was derived using the bicubic spline surface described in the next section. Local slopes with the BLF were calculated for 12 directions spaced at 30° intervals centered on the nadir point. The maximum slope value and direction were used to estimate a first order correction (P.K. Chua, unpublished M.Sc. thesis, 1989).

Terrestrial Height Data Set

Terrestrial height data in a convenient format and with a sufficient coverage are essential for this study to provide "ground truth." Ideally, we need heights to better than the expected precision of the altimeter, i.e., to better than about 10 cm. After investigation we found that the height values in the Australian National Gravity Data Base (AGDB) gave the best available coverage, although on the whole failed to meet our precision specifications. The AGDB is held and maintained by the Bureau of Mineral Resources, Geology and Geophysics (BMR), Australia, and is available on magnetic tape to outside agencies. It was supplied free of charge to MSSL by the BMR for the purposes of this investigation.

The information on the AGDB includes the station's geodetic latitude and longitude, gravity, and height (m) at every gravity station occupied. Gravity stations are observed on (at least) an 11-km grid, and the coverage is practically complete onshore, giving a data set of over 450,000 points. Figure 5 shows the distribution of the gravity stations over the project area.

The height values in the AGDB are generally defined on the Australian Height Datum (AHD), the official vertical datum for Australia. It is defined by a least-square adjustment of, mainly, third-order spirit leveling, tied to mean sea level (MSL) as defined by 30 tide gauges spaced evenly around the coastline of the continent. Consequently, heights within the AGDB may be treated as orthometric heights. Unfortunately, because the siting of some of the tide gauges was poor, the estimation of MSL by constraining each gauge to zero means that the AHD is not a true equipotential surface, and may depart from a geoid by up to a few metres. (Steed, 1989, personal communication). This could introduce a bias of this order in any estimation of accuracy which uses these heights as control.

Most of the height values in the AGDB were found by barometric leveling, with an accuracy in the range of ±4 to ±6 metres (Barlow, 1977). Occasionally, theodolite stadia traverses were used to provide more precise height control in areas of special geophysical interest. In such cases, the precision of the point heights is expected to be better than ±30 cm. Examples of such traverses show up in Figure 5 as the intensive linear patterns in the northwest and east of the area, whereas the barometrically derived height points are the evenly space background grid covering the same area.

A digital elevation model was created within the study area based on the original height data by fitting a bicubic spline surface to the pseudo-regularly distributed orthometric BMR heights, i.e., the height values taken from the AGDB. The nature of the bicubic spline surface is such that it is well suited to the generally smooth terrain encountered in the study area, and is a powerful tool with which to estimate mean heights. The fitting procedure used first subdivides the project area into smaller squares called panels. Separate bicubic spline surfaces joined with continuity up to the second derivative across the panel boundaries are then computed by minimal, weighted least-squares fitting. This gives a continuous surface description of

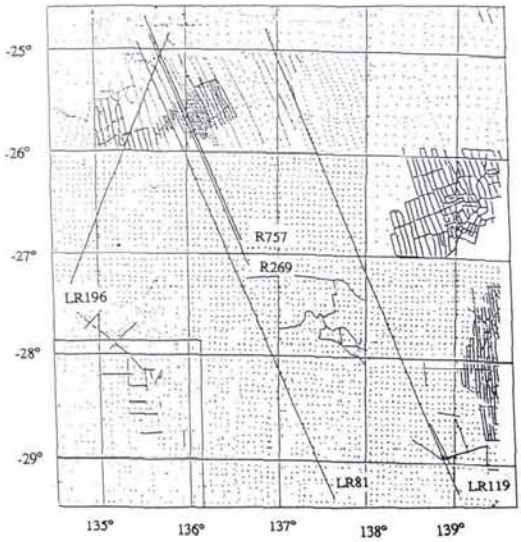

FIG. 5. Distribution of height points from BMR gravity stations and Seasat ground traces for LR81, LR119, LR196, R269, and R757.

the terrain within the project area (Hayes and Halliday, 1974; Numerical Algorithms Group, 1988).

The project area was subdivided into 1,600 panels with sides of 0.125° (~14 km). With 18,035 gravity stations in the same area, an average of around 11 orthometric height values were used in the determination of each bicubic spline surface. A root-mean-square (RMS) value of 4.65 m was computed for the fitting of the bicubic spline surface to the BMR heights, after outlier removal. Figure 6 shows the histogram for the height differences between the bicubic spline defined heights and their corresponding BMR height values (P.K. Chua, unpublished M.Sc. thesis, 1989).

Comparison of Altimetrically Derived Orthometric Heights with Control Data

To compare the Seasat altimeter-derived orthometric heights (H_{alt}) with the BMR heights, (H_{BMR}) we define:

$$H_{diff} = H_{BMR} - H_{alt}. \quad (6)$$

Substituting Equation 4 into Equation 6, we have

$$H_{diff} = H_{BMR} - \{h_{sat} - ([R_m + \delta R]S + \Delta h_{Etide} + N_{model})\}. \quad (7)$$

The values of H_{diff} will contain contributions from errors in

- the determination of satellite heights above the reference ellipsoid,
- the measurement of altimeter ranges and the determination of its corrections,
- the determination of the geoidal undulations,
- the BMR heights, and
- the fitting of the bicubic spline to the BMR heights.

The height difference can be considered in terms of a "signal" component, and a "noise" component, made up from various elements of the error contributions summarized above, depending upon their spatial wavelengths. H_{diff} may thus be expressed as

$$H_{diff} = \Delta H_{syst} + \Delta H_{rand}. \quad (8)$$

A least-squares regression line was used to model H_{diff}, thus allowing the analysis of H_{diff} in terms of its systematic and random components. By investigating the ΔH_{syst} component, we may investigate the main contributors to the *accuracy* of H_{alt}, and by studying ΔH_{rand}, we can learn about those elements which influence the *precision* of H_{alt}.

Note that, hereafter, all reference to height means orthometric height, unless stated otherwise.

Details of the Case Study

The area chosen for the test was described earlier. As shown in Figure 6, we identified five Seasat tracks (LR81, LR119, LR196, R269, and R757) as possible subjects for study. As an exercise, a total of seven combinations of orbit models and geoidal undulations (derived from different geopotential models) were evaluated, and it was found that the best results came when using GEM-T1 for orbit modeling, and OSU86E for geoid evaluation (P.K. Chua, unpublished M. Sc. Thesis, 1989).

We narrowed the study down further by first concentrating on track LR81. For this track, about 216 km of 14 contiguous blocks (blocks 1506 to 1519) of altimeter data were used. This gave 218 echoes after simple waveform filtering, which rejected 13 percent of the waveforms in the test area. These rejected waveforms are seen to be contaminated by bright targets in the footprint (possibly clay pans). A profile for this track from both the Seasat altimeter-derived and spline-fitted data is shown in Figure 7, which covers a range in height of about 260 m. The values of the effective slope (in decimal degrees) of the terrain within the beam limited footprint of the Seasat altimeter along the profiles are also shown.

The results of the comparisons (H_{diff} – Equation 7) are plotted in Figure 8. The RMS of height differences before the removal of the trend is 2.6 m. After removing a trend of bias about 1 m and tilt of −5.5", the RMS value of the differences reduces to 1.9 m.

Certain features of Figure 8 deserve special mention.

(i) It can be seen that the height differences seem to fall into groups, or bins, according to their biases and amplitudes. The biases for the first two-thirds of the profile range from about 2 to 4 m, with amplitudes of a few metres. In contrast, the bias for the last third of the profile is about −1 m, with an amplitude of about one metre. One is led to suspect from such behavior that we are considering two distinct populations of data in this profile. The contributors to errors in H_{diff} have been summarized above, but because of the discontinuous behavior of the bias, we attribute this phenomenon to errors in the levelling, i.e., in the values of H_{BMR} used for control. A check with Figure 5 confirms this suspicion. For most of its path, the track for LR81 crosses areas where the heights are obtained by barometric leveling. Near the end of the path, where the H_{diff} are significantly smaller, the track enters an area where the height points are arranged in linear patterns, and were evidently obtained for an intensive gravimetric and seismic survey. This presumption is confirmed by a map of the region, covering McDills, Northern Territory (Division of National Mapping, 1962). As noted earlier, in such surveys, heights are obtained by theodolite traversing using a stadia technique. This should give precision in height to better than ±30 cm, compared with the several metres expected

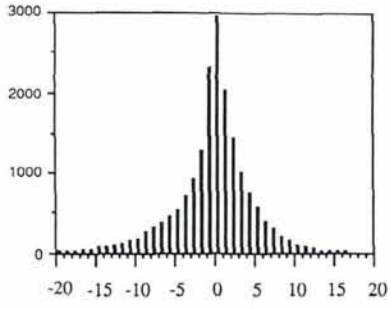

FIG. 6. Histograms of residuals (m) from bicubic spline fitting to BMR height data.

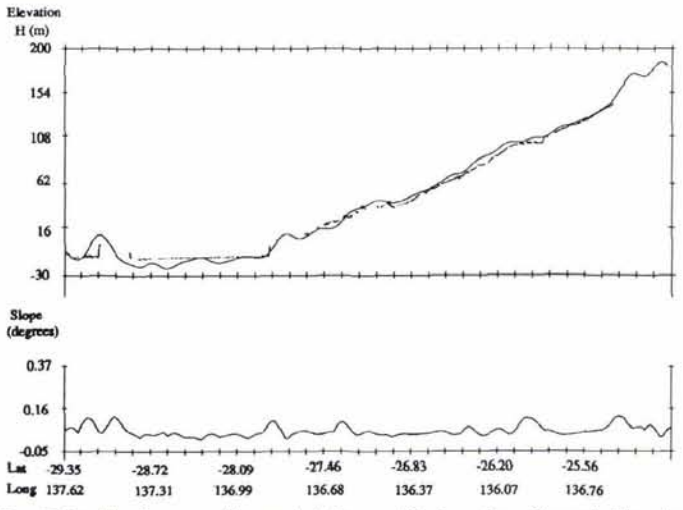

FIG. 7. Profiles for LR81. Upper plot: Ground Surface from Seasat altimetry (broken line) and bicubic spline fitted to BMR height data. Lower plot: Effective slope value along bicubic spline profile.

from heights obtained using barometric leveling. In other words, where the superior height control is encountered, the orthometric heights recovered from the satellite altimetry fit the control better.

(ii) The H_{diff} fluctuations have half wavelengths roughly equal to the size of the panels used during the fitting of bicubic spline to the BMR heights, so could possibly reflect the low order of the spline fitting. They may also reflect the "footprint" of the gravity campaigns, which cover the ground in an interlocking, cloverleaf pattern and whose day-to-day characteristics may vary according to, e.g., variations in atmospheric conditions.

(iii) If the biases in the H_{diff} result from systematic errors in the barometrically derived height values, as seems most likely, this has serious repercussions in those branches of the geodetic and geophysical sciences which use digital elevation models. For example, precise geoid computations which use DEMs to compute free air gravity anomalies are far more tolerant of relatively large (±3 mGal) random errors in the gravity data than they are of smaller systematic errors. A systematic error of 4 m in height gives an error of 1.2 mGal in the gravity anomaly. Over the wavelengths seen in Figure 8, such a bias produces an error of about 1 to 2 ppm in the geoidal height differences computed from gravimetry (Kearsley, 1986), significantly degrading the expected precision of such evaluations.

Comparison with Higher-Order Control

We have noted the improved agreement of H_{alt} with the control when the LR81 track enters an area of superior height control. In order to obtain a more realistic estimate of the potential accuracy of the satellite altimeter, we decided to analyze in detail the results in this area. In Figure 9 we show the raw BMR height distribution at 1842 locations over this region, bounded approximately by $-25.37° \leq \varphi \leq -25.87°$ and $135.5° \leq \lambda \leq 136.5°$ (equivalent to 4 by 8 bicubic spline panels). Figure 9 also shows the Seasat tracks LR81 and R757 used in this case study. The two tracks are separated by a distance of about 24 km and cross the Simpson Desert from south to north. Three contiguous blocks of data from each of the two tracks are assessed, giving, after waveform editing, 60 and 63 useable returns from LR81 and R757, respectively. Each profile covered a distance of over 46 km. The behavior of the geoid along these profiles has been described earlier.

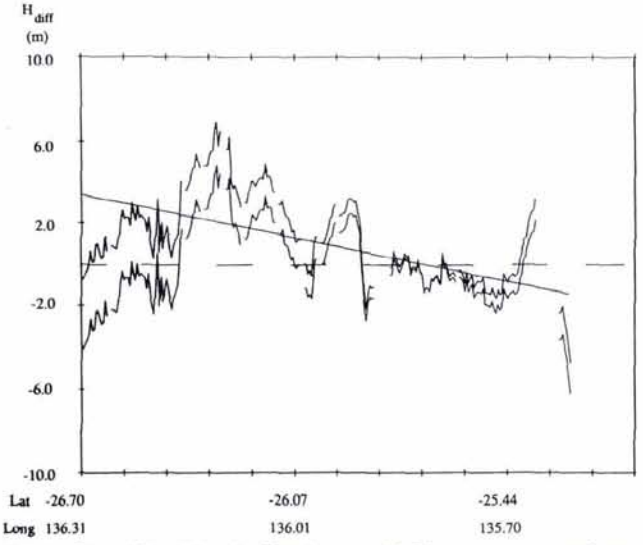

FIG. 8. Signal Modeling for Track LR81. (a) The upper curve shows height differences before the trend is removed. (b) the lower curve after the trend is removed. The solid straight line shows the regression line fitted to (a).

(i) Digital Elevation Modeling. The RMS of the fitting of a bicubic spline to raw BMR heights in this region is about ±3 m, an indication of the smoothness of this terrain. The average number of height points per cubic spline panel is about 55, and from this we infer that the spline surface can recover the mean height of the area covered by the panel to a precision of about ±0.4 m. We use this value to estimate the noise level in the heights calculated from the bicubic spline surfaces in this test.

(ii) Results of Comparisons. The results of the comparisons for these profiles are plotted in Figures 10 and 11, and summarized in Table 1. For LR81 the RMS of the H_{diff}, before removal of any trend, is ±1.1 m. The same statistic for R757 is ±1.5 m. (This latter comparison was performed using PGS-S3, the geopotential model supplied with the altimetry data for the orbit model (Lerch *et al.*, 1982, p. 3286) as GEM-T1 was unavailable for this track. However, our experience in this study has shown that PGS-S3, although less reliable than GEM-T1, was still capable of producing useable results (see P.K. Chua, unpublished M.Sc. thesis, 1989). The linear trends, characterized by a bias of −0.82 m and slope of −1.1″ for LR81, and a bias of −0.78 m and a slope of +0.3″ for R757 (see Table 1), were removed and the analysis repeated, giving an RMS of ±0.4 m for LR81 and ±0.7 m for R757.

(iii) Differences between Tracks. The comparison of the LR81 track is significantly better than that for R757. The reason for this may be explained partly by the use of GEM-T1 to model the orbit for LR81, compared with PGS-S3 which was used to model R757's orbit. It may also be explained by the fact that the track for LR81 fits the theodolite traverse providing the height control almost exactly, whereas the ground track for R757 starts between two traverses in the south, and crosses the eastern traverse as it travels north (see Figure 9). Because of this poorer coincidence for R757, we feel that the results from the LR81 comparison may give the more realistic estimate of the true capability of the altimeter.

DISCUSSION OF RESULTS

Accuracy and Precision of Seasat Altimetry

We have noted that there was a bias of about −0.8 m in H_{diff} for both LR81 and R757. This implies that, if we use GEM-T1 or PGS-S3 for orbit modelling and OSU86E for geoid modelling, the mean height recovered from Seasat altimetry for this profile is *accurate* to slightly better than 1 m. When the trend in H_{diff} is removed for LR81, an RMS value of about ±0.4 m for an individual height estimation is obtained. With 60 altimeter returns used to determine the profile, this gives a *precision* of about ±5 cm for the mean, i.e., for the fit of the altimeter track to the whole profile. The RMS value for R757 after trend removal is about ±0.7 m. The precision for the profile in this case is, from 63 altimeter returns, around ±8 cm.

TABLE 1. RESULTS OF ANALYSIS OF H_{diff} FOR TRACKS LR81 and R757

Track	LR81	R757
No. of returns	60	63
Before removal of trend		
RMS of H_{diff} (point value)	±1.1m	±1.5m
After removal of trend		
RMS of H_{diff} (point value)	±0.41m	±0.66m
RMS of H_{diff} (for mean value of the 46 km profile)	±0.05m	±0.08m
Trend line details		
Bias	−0.82m	−0.78m
Slope	−1.1″	0.3″

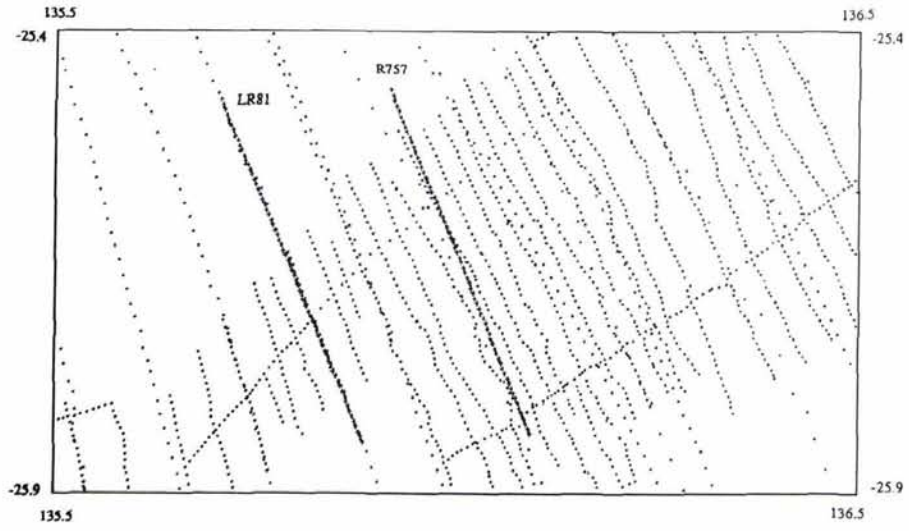

FIG. 9. Ground tracks of LR81 and R757 over detailed study area. + – Nadir point for altimeter pulse. ◇ - Height points at BMR gravity stations.

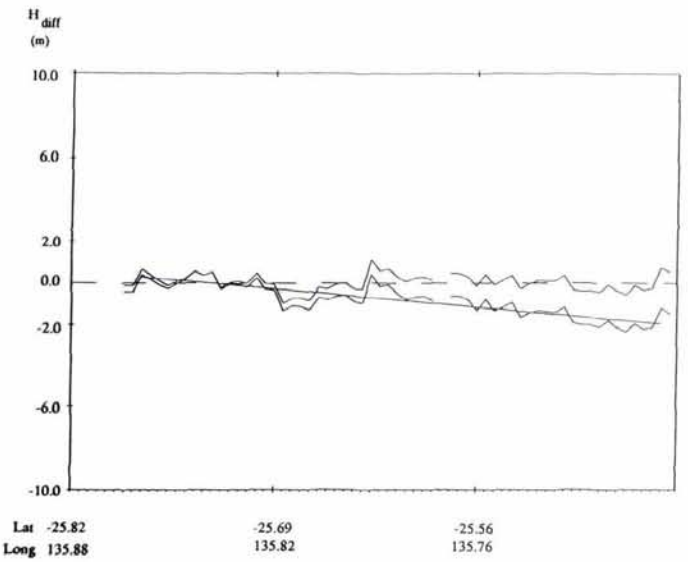

FIG. 10. Signal Modeling for the selected section of Track LR81. (a) The lower curve shows height differences before the trend is removed, (b) the upper curve after the trend is removed. The solid straight line shows the regression line fitted to (a)

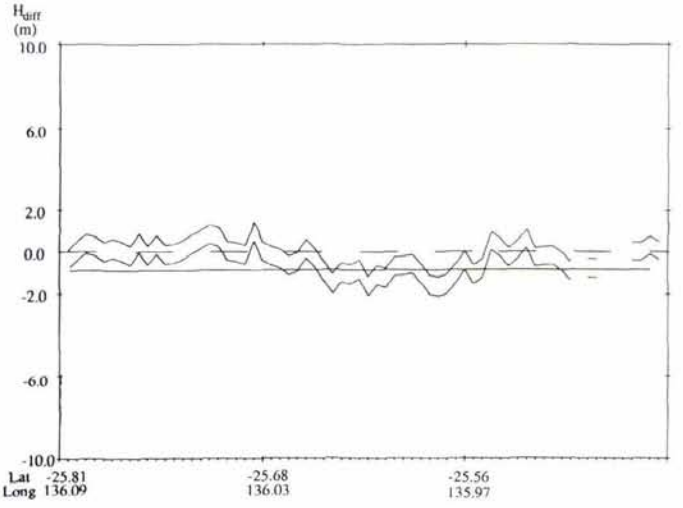

FIG. 11. Signal Modeling for the selected section of Track R757. (a) The upper curve shows height differences before the trend is removed, (b) the lower curve after the trend is removed. The solid straight line shows the regression line fitted to (a)

ERROR CONTRIBUTORS

Contributions to ΔH_{rand}

The factors which may introduce errors into the height determination are listed earlier. In view of the length of the tracks analyzed, the "noise" component of H_{diff}, i.e., ΔH_{rand}, may be attributed to

- altimeter instrument noise (estimated to be about 3 cm),
- "noise" in bicubic spline representation of BMR heights (estimated in the Details of the Case Study section to be about ± 0.4 m), and
- noise in the surface bias correction (not known).

Random errors may also result from errors in the models used to estimate, i.e.,

- atmospheric propagation corrections (estimated to be about 2 cm),
- slope correction (we estimate an average effective slope value of 0.05°, with an error of $\pm 0.005°$, gives an error of about 0.06 m, taking 800 km as the satellite height above the reference ellipsoid),
- retracking corrections (error unknown),
- Earth tide corrections (error unknown), and
- errors in the geoid heights from OSU86E (computed along the profiles at about 5cm).

The known sources of "noise" above give an estimated RMS value of ± 0.4 m, which matches the precision obtained in the comparison for LR81. We therefore expect the magnitude of the unknown "noise" terms above to be at the centimetre level, at most. Consequently, most of the apparent contribution to the noise in ΔH_{rand} comes, not from the altimetry, but from the estimation of the heights used as control in the test.

Contributions to ΔH_{syst}

We now consider the factors which contribute to the (a) bias and the (b) tilt in the systematic component of H_{diff}, i.e., to ΔH_{syst}.

(a) Bias. This group of factors includes

(i) residual altimeter instrument bias (expected to be about a centimetre (Francis *et al.*, 1989)),

(ii) liquid tropospheric bias (by leaving out the liquid tropospheric correction, a bias of around -5 cm is introduced),

(iii) residual retracking bias (analysis of the waveforms returned along a selected altimeter profile, taking into consideration the retracking

algorithm used, should yield an estimate for the residual retracking bias),
(iv) surface bias (with the development of a surface model for the terrain type concerned, an estimate for the surface bias will be available),
(v) bias in the reference geoid, and
(vi) mean orbit bias.

The main contributors to the bias are (iv), (v), and (vi). Of these, only (vi) comes from the altimetric component in the comparison. Given that AHD is known to contain biases of 1 to 2 m, it is quite probable that the major fraction of the bias in the comparison comes from the height control. If this is the case, it follows that the altimeter component of the comparison has been well determined from the orbit models in this test area.

The bias in the orbit is difficult to determine, because the tidal model is inadequate over these parts of the orbit. In the case of R757, the ocean bias to the south is about −2.2m and to the north about +1.6m. However, because of the likely bias in the height of the ground control, it is difficult to establish any meaningful estimate of the orbit bias from this test.

It is important to note the value of using a good geoid model in recovering the orthometric heights from the h_{sat}. If GEM-T1 is used instead of OSU86E to calculate the N value in Equation 4, the RMS of H_{diff} is unchanged, but the bias term becomes +3.72 m (P.K. Chua, 1989, unpublished M.Sc. Thesis). In all combinations of models tested, N values derived from OSU86E summed to degree and order 360 proved to give the smallest bias. A comparison of OSU86E against the most recent high-order OSU89A (Rapp, 1990, personal communication), which is based upon GEM-T2, shows little bias in the former in this region. However, biases of up to 3m do exist between the two models in the Australian region (Kearsley and Govind, 1990). For the most accurate values of H from altimetry, evidence to date suggests the more recent OSU89A or B should be used as the reference model for N determinations.

(b) Tilt. Terms which contribute to tilt include the slope of the reference geoid model with respect to a true equipotential, and the slope in the radial orbit determination.

From Figures 10 and 11, one can see that the slope of the fitted first-order polynomial to LR81 is greater than the slope of the trend line for R757. Over a distance of about 46 km along the ascending LR81 track, the altimeter-derived orthometric heights *increase* by about 2.5 m with respect to the H_{BMR}. Over the same distance, the H_{alt} values from R757 *decreased* by about 0.23 m with respect to the BMR heights. Such a change in the slope does not come from a change in geoid slope, and is probably an indication of the difference in the tilt of the computed orbits for the two tracks, resulting from the different models used. In fact, from R757 measurements over the ocean south and north of Australia, we find that the slopes of the orbit are, respectively, 1.8e-5 and -5.3e-5. These are compatible with the values over Simpson Desert, which were -0.5e-5. The distance scale for this change in slope is reasonable, and the change is in the correct direction throughout this part of the orbit.

Implications and Applications

From the discussion above, we infer that mean terrain heights, for relatively smooth areas, may be recovered to a precision of at least ±40 cm for an individual range. This precision can be greatly improved if profiles rather than individual heights are determined. As a result we suggest that satellite altimetry could be used for a number of different applications, depending upon which part of the heighting "equation" is known. These applications are listed below.

(i) In its most direct application, and where the terrain allows, the altimeter can be used to provide accurate digital evaluation models (DEMs), or to check or upgrade existing DEMs. The experience from these tests strongly suggests that serious biases exist in the DEM derived from the Australian Gravity Data Base. These biases could significantly degrade any computation based on this DEM (e.g., precise regional geoid solutions).
(ii) One of the main limitations to oceanographic applications of satellite altimetry is the knowledge of the orbit. Provided the altimeter is calibrated and the ellipsoidal heights of the land surface are known, altimetry over surfaces such as that in the study area could be used as a pseudo-range in the observation equations used to determine the orbit ephemeris. Using profiles such as those in the study, the orbit could be constrained to ±5 cm over some parts of the globe which at present lacks satellite tracking facilities. Such an application would provide ranging information for each pass, which would greatly enhance the orbits, and in turn improve the derivation of ocean heights used in oceanographic studies.
(iii) Conversely, the technique can be used to find the geoid undulation over the area covered by the satellite track. In this configuration, ellipsoidal heights are derived from the altimeter over areas of known orthometric heights, and the geoid-ellipsoid separations are determined from Equation 2. This could be used to enhance the geoid model in those areas where insufficient gravity data exists to allow a precise gravimetric solution.

CONCLUSIONS AND RECOMMENDATIONS

As a result of the research reported above we feel we can draw the following conclusions:

(i) Bi-cubic spline-fitting to heights over areas of smooth terrain provides a good terrain model, giving estimates of mean heights to about ±0.4 m for areas of 0.125° square.
(ii) It appears that satellite radar altimetry can recover terrain heights over smooth terrain to a precision of about ±0.4 to 0.7 m per range. The precision along a profile of three contiguous blocks of range data is about ±5 to ±7cm.
(iii) The bias term in the height comparison was 0.8 m, which implies the accuracy of the altimeter is at about this level. However, it is recognized that the height used for control in the study suffers systematic errors which could easily be of this size, so the actual accuracy may be much better. It was also apparent from the tests that this 0.8-m agreement could only be achieved if one of the recent high order geopotential models was used to provide the geoid height. Such a model should be used to transform the altimetry-derived ellipsoidal heights to orthometric heights, although for highest accuracy a detailed analysis of the local gravity field should also be included in the geoid height evaluation.
(iv) As a consequence of (ii) and (iii), altimetric ranges over smooth areas of known height could be used to calibrate the radar altimetry at the 5- to 7-cm level.
(iv) Depending upon the configuration of known parameters, radar altimetry over regions of known height could be used to provide range data for orbit improvement. This could have far-reaching benefits for all users of satellite radar altimetry.
(v) The test shows that satellite altimetry can measure heights over relatively smooth terrain to sub-metre precision. This technique could prove to be enormously beneficial in providing estimates of mean heights for topography, especially in areas where conventional mapping techniques are too expensive, or simply inadequate. Where the terrain allows, altimetrically derived heights can be used to test and/or extend digital elevation models. This study suggests that significant biases exist in the height data used for control. Such biases will propagate as systematic errors into all studies based upon them, e.g., detailed geoid studies.

ACKNOWLEDGMENTS

We gratefully acknowledge the assistance of the Algorithm Development Facility of the UK Earth Observation Data Centre in preparing some of the altimeter data sets. We are also most grateful to the Australian Bureau of Mineral Resources, Geology and Geophysics for the provision of digital height data from the Australian Gravity Data Base, without which this research would not have been possible. Major contributors to this data

base were the Department of Mines in New South Wales, South Australia and Tasmania, the University of Tasmania, and West Australian Petroleum Pty. Ltd.

REFERENCES

Andrewartha, R., R. Durrant, C. Cudlip, M. Guzkowska, C. G. Rapley, J. Ridley, H. D. Griffiths, D. J. Wingham, J. Bradford, R. J. Powell, and P. Sohtell, 1988. An Advanced Terrain Tracking Altimeter. *Proc. of IGARSS'88 Symp.*, Edinburgh, Scotland, Sept 1988, pp. 969–972.

Barlow, B. C., 1977. Data limitations and model complexity; 2-D gravity modelling with desk-top calculators, *Bull. Aust. Soc. Explor. Geophys.*, Vol. 8, No. 4, pp. 139–143.

Brenner, A. C., R. A. Bindschadler, R. H. Thomas, and H. J. Zwally, 1983. Slope-induced errors in radar altimetry over continental ice sheets., *J. Geoph. Res.*, Vol. 88, No.C3, pp. 1617–1623.

Division of National Mapping, 1962. *Map SG 53-7* (McDills, Northern Territory). Distributed by Department of National Development, Canberra, Australia.

Francis, C. R., and B. Duesmann, 1989. *ERS-1 Altimeter Calibration.* ESTEC Ref. ER-TN-ESA-RA-0003, ESTEC, Noordwijk, Holland.

Griffiths, H. D., 1984. Special difficulties of retrieving surface elevation over continental ice, *Proc. of Workshop on ERS-1 Radar Altimeter Data Products,* Frascati, Italy, May 1984, pp. 61–65.

Guzkowska, M., W. Cudlip, C. R. Rapley, and J. K. Ridley, 1989. *Developments in Inland Water and Land Altimetry,* Final Report, ESA contract No. 7839/88/F/Fl.

Hartl, P., 1984. The Precise Range and Range Rate Equipment (PRARE) and its possible support to the radar altimeter measurements for ERS-1, *ERS-1 Radar Altimeter Data Products,* ESA SP-221, pp. 153–160.

Hayes, J. G., and J. Halliday, 1974. The least squares fitting of cubic spline surfaces to general data sets, *J. Inst. Maths Applics,* Vol. 14, pp. 89–103.

Heiskanen, W. A., and H. Moritz, 1967. *Physical Geodesy,* W. H. Freeman, 364 p.

Jet Propulsion Laboratory, 1980a. *Seasat Altimeter Geophysical Data Record (GDR) User Handbook,* NASA.

———, 1980b. *Seasat Altimeter Geophysical Algorithm Specifications,* NASA.

Kearsley, A. H. W., 1986. The determination of precise geoid height differences using ring integration, *Boll. Sci. Affini,* Anno XLV, No. 2, pp. 151–174.

Kearsley, A. H. W., and R. D. Holloway, 1988, Geopotential models in the Australian region, *Proc. A. G.U. Chapman Conf. on Progress in the Determination of the Earth's Gravity Field,* Fort Lauderdale, Florida, 13-16 Sept., pp. 23–26.

———, 1989. Tests on geopotential models in the Australian region. *Aust. J. Geod Photogram. Surv.*, No. 50, pp. 1–17.

Kearsley, A. H. W., and Ramesh Govind, 1990. The Australian Geoid - status and problems, Presented at the First Symposium of the International Geoid Commission, Milan, 11-14 June 1990.

Lerch, F. J., Marsh, J. G., Klosko, S. M. and Williamson, R. G., 1982. Gravity model improvement for SEASAT, *J. Geophys. Res.*, Vol. 87, No. C5, pp. 3281–3296.

Marsh, J. G., F. J. Lerch, B. H. Putney, D. C. Christodoulidis, D. E. Smith, T. L. Felsentreger, B. V. Sanchez, S. M. Klosko, E. C. Pavlis, T. V. F. Martin, N. L. Chandler, K. E. Rachlin, G. B. Patel, S. Bhati, and D. S. Chinn, 1988. A new gravitational model for the earth from satellite tracking data: GEM-T1, *J. Geophys. Res.*, Vol. 93, No. B6, pp. 6169–6215.

Moritz, H., 1980. Geodetic Reference System 1980. *Bull. Géod.* Vol. 54, No. 3, pp. 395–405.

Numerical Algorithms Group, 1988. *NAG Fortran Library Manual,* Numerical Algorithms Group Ltd (NAG), U.K., Mark 13, Vol. 3.

Rapley, C. G., and H. D. Griffiths, 1984. Modelling of altimeter tracking over topographic surfaces. *Proc. of Workshop on ERS-1 Radar Altimeter Data Products,* Frascati, Italy, May 1984, pp. 177–180.

Rapley, C. G., M. A. J. Guzkowska, W. Cudlip, and I. M. Mason, 1987. *An Exploratory Study of Inland Water and Land Altimetry Using Seasat Data,* ESA Contract Report 6483/85/NL/BI.

Rapp, R. H., and J. Cruz, 1986. *Spherical Harmonic Expansions of the Earth's Gravitational Potential to Degree 360 Using 30' Mean Anomalies,* Report No. 376, Dept of Geod. Sci. and Surv., The Ohio State University, Columbus, Ohio.

Ridley, J. K., 1989. The topography and surface characteristics of the Larsen Ice Shelf, Antarctica, using satellite altimetry, *J. Glaciology,* Vol. 35, No. 121, pp. 299–310.

Wingham, D. J., C. G. Rapley, and M. D. Griffiths, 1986. New techniques in satellite altimeter tracking systems, *Proc. IGARSS Symposium,* Zurich, Switzerland.

(Received 11 January 1990; revised and accepted 2 July 1990)